A GLOBAL ANALYSIS OF DIFFRACTIVE EVENTS AT HERA

SARA TAHERI MONFARED
ALI KHORRAMIAN

Semnan University &
School of particles and accelerators,
Institute for Research in Fundamental Science (IPM)

A GLOBAL ANALYSIS OF DIFFRACTIVE EVENTS AT HERA

- Motivation
- DIS & DDIS phenomena
- Introduction of different diffractive data sets
- Global fit procedure
- Results and conclusion

Motivation

- Structure functions are a measure of the partonic structure of hadrons, which is important for any process which involves colliding hadrons.

- **They are key ingredient for deriving PDFs in nucleons**.

- These PDFs allow us to predict scattering cross sections at particle colliders. A good knowledge of PDFs is of prime importance for the success of the physics program.

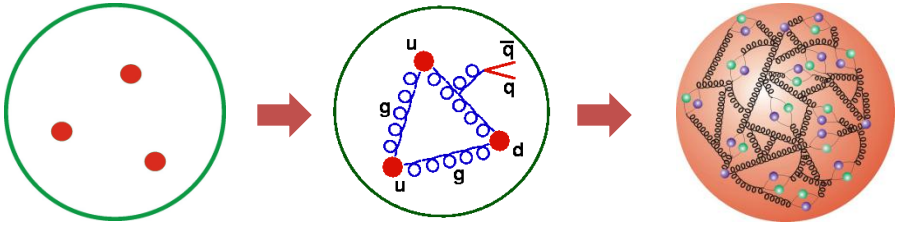

A. De Roeck and R. S. Thorne, arXiv:1103.0555 [hep-ph].

M. G. Albrow *et al.* [FP420 R and D Collaboration], JINST **4**, T10001 (2009) [arXiv:0806.0302 [hep-ex]].

Motivation

The H1 and ZEUS collaborations presented their results on inclusive and various exclusive reactions, which is being actively studied by theorists and give access to a broader understanding of proton structure.

Although data-taking there has been stopped, new results continue to appear.

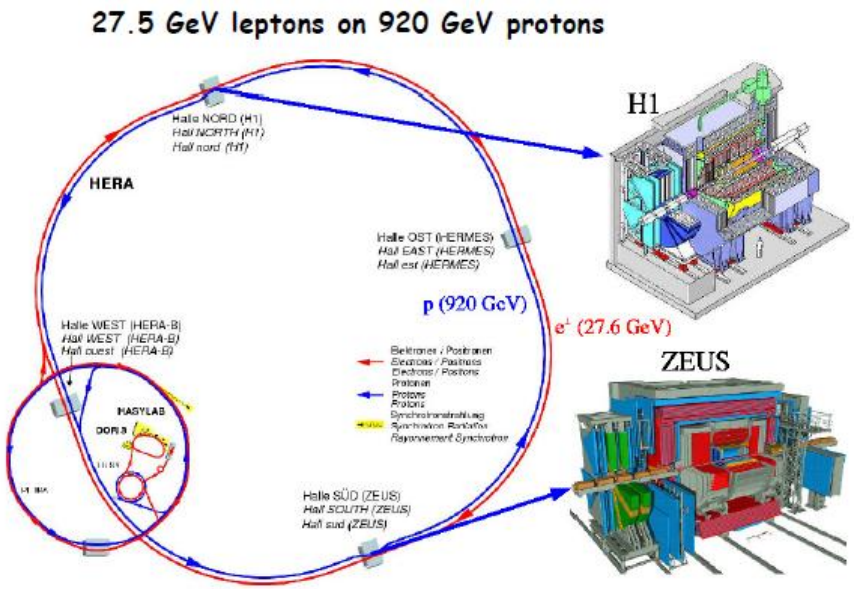

H. Collaboration, arXiv:1010.1476 [hep-ex].

DIS and DDIS

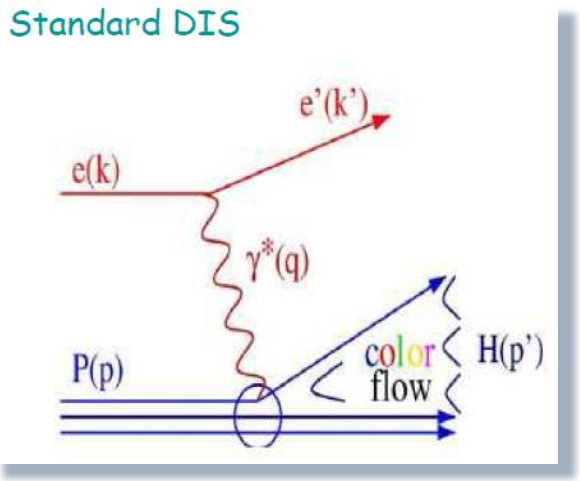

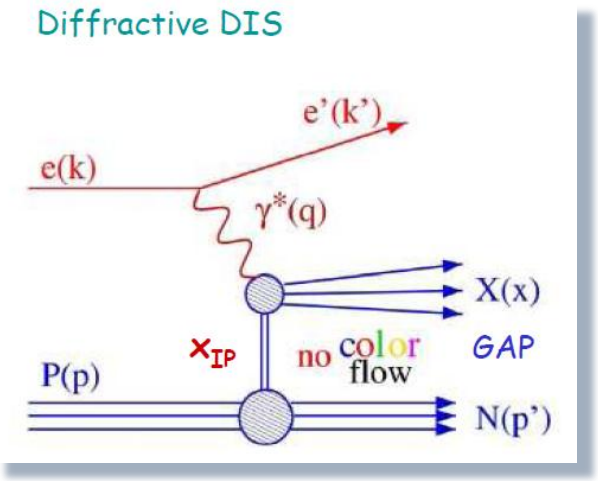

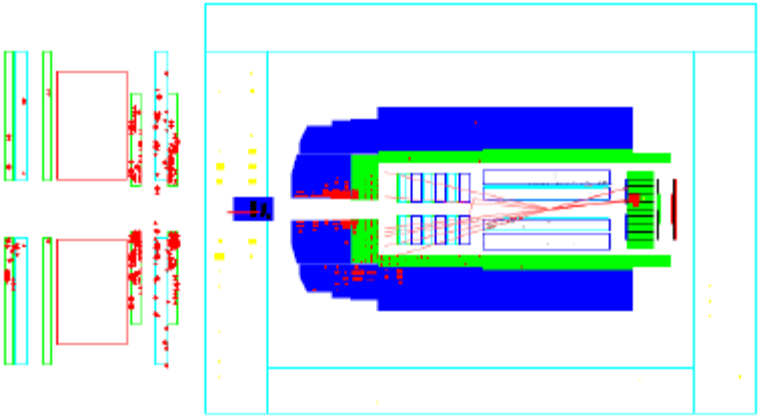

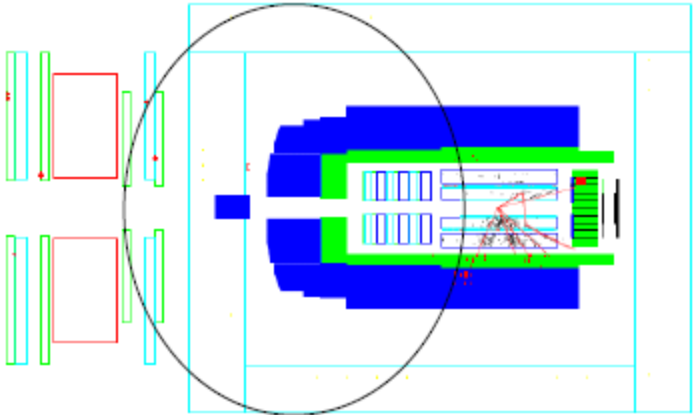

Approximately 10% of DIS phenomena are of diffractive nature

DIS kinematics

Before the proper analysis we need to define the usual kinematic variables. The main variables used for the description of DDIS are similar to the those of DIS variable.

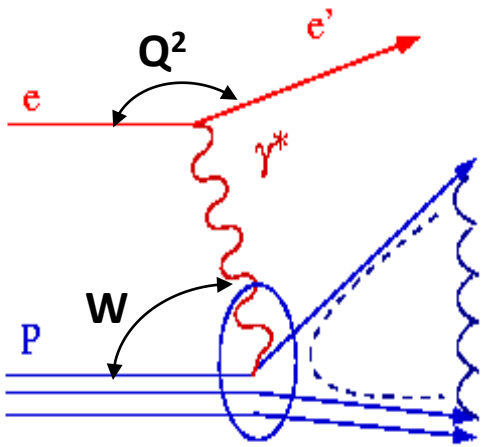

Q^2 = virtuality of photon
=(4-momentum exchanged at e vertex)^2

W = invariant mass of photon-proton system

x = Bjorken's variable for the Proton
= fraction of Proton's momentum carried by struck quark

y = inelasticity

DIS probes the partonic structure of the proton

$$\frac{d^2\sigma}{dxdQ^2} = \frac{4\pi\alpha^2}{xQ^4}\left\{1 - y + \frac{y^2}{2[1+R(x,Q^2)]}\right\}F_2(x,Q^2)$$

DDIS kinematics

The variables related to DDIS bear a close resemblance to the those of DIS.

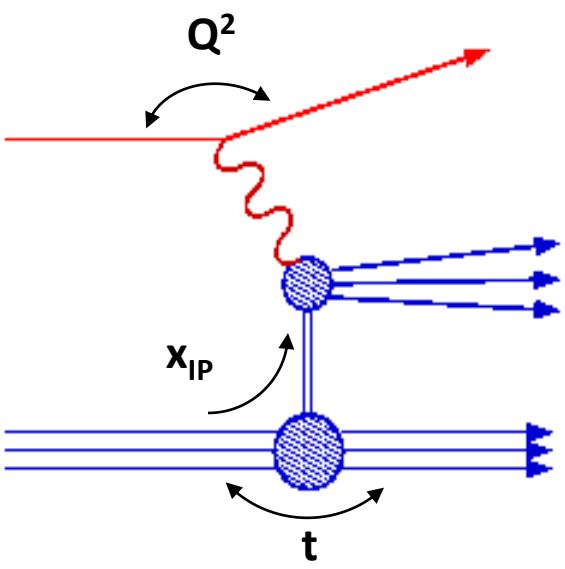

x_{IP} = fraction of proton's momentum taken by Pomeron

β = Bjorken's variable for the Pomeron
= fraction of Pomeron's momentum carried by struck quark
$= x/x_{IP}$

t = (4-momentum exchanged at p vertex)^2
typically: $|t| < 1\text{GeV}^2$

M_X = invariant mass of photon-Pomeron system

$$\frac{d^4\sigma}{d\beta dQ^2 dx_{IP} dt} = \frac{4\pi\alpha^2}{\beta Q^4}\left\{1 - y + \frac{y^2}{2(1+R^{D(4)})}\right\} F_2^{D(4)}(\beta, Q^2, x_{IP}, t)$$

Theoretical basis of our analysis

Regge

There are 4 different theoretical approaches to analyze diffractive data:

1) The Pomeron structure function (PSF) model formulated in the framework of Regge phenomenology
2) The the Bartels-Ellis-Kowalski-Wusthoff (BEKW) two gluon exchange dipole model
3) The Bialas-Peschanski (BP) model based on the BFKL Pomeron approach
4) The saturation model of Golec-Biernat and Wusthoff (GBW)

These four frameworks are based on completely different theoretical concepts. The best description of all available measurements can be achieved with either the PSF based model or the BEKW approach.

Diffractive cross sections

The data are often presented in the form of a t-integrated cross section

$$\frac{d^3\sigma^{ep\to eXY}}{\mathrm{d}x_{I\!P}\ \mathrm{d}\beta\ \mathrm{d}Q^2} = \frac{4\pi\alpha^2}{xQ^4}\left(1-y+\frac{y^2}{2}\right)\sigma_r^{D(3)}(x_{I\!P},\beta,Q^2)\ ,$$

or in terms of a diffractive structure function

$$\sigma_r^{D(3)} = F_2^{D(3)} - \frac{y^2}{Y_+}F_L^{D(3)}$$

$$Y_+ = 1+(1-y)^2$$

can be neglected anywhere but at very large y

$$sxy = Q^2$$

Longitudinal structure function plays an important role in low-x physics

QCD (collins) factorization

PHYSICAL REVIEW D VOLUME 57, NUMBER 5 1 MARCH 1998

Proof of factorization for diffractive hard scattering

John C. Collins*
Penn State University, 104 Davey Lab, University Park, Pennsylvania 16802
(Received 14 October 1997; published 6 February 1998)

A proof is given that hard-scattering factorization is valid for deep-inelastic processes which are diffractive or which have some other condition imposed on the final state in the target fragmentation region.
[S0556-2821(98)00507-4]
PACS number(s): 13.85.Ni, 12.38.Aw, 13.60.−r

$$\mathrm{d}\sigma^{ep\to eXY}(x,Q^2,x_{I\!P},t) = \sum_i f_i^D(x,Q^2,x_{I\!P},t) \otimes \mathrm{d}\hat{\sigma}^{ei}(x,Q^2)$$

It implies that the cross section for the diffractive process can be written in terms of convolution of DPDFs with universal partonic cross sections.

Proton vertex factorization

The proton vertex factorization framework, in which the DPDFs are factorized in to a term depending only on X_{IP} and t and a term depending only on β and Q^2, is often assumed:

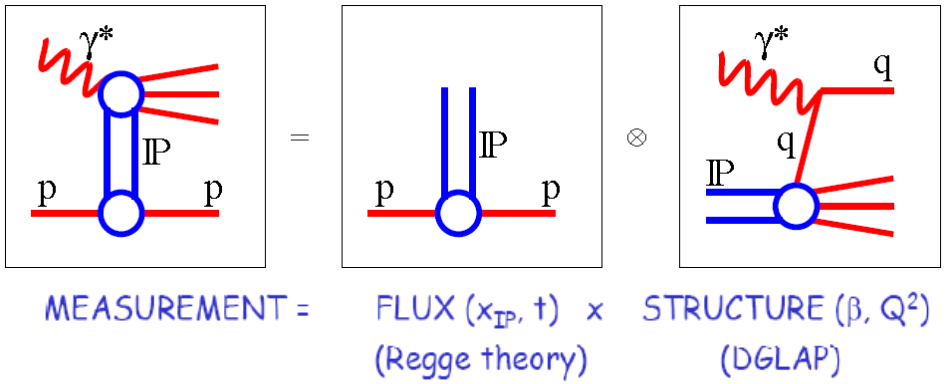

$$f_i^D(x, Q^2, x_{\mathbb{P}}, t) = f_{\mathbb{P}/p}(x_{\mathbb{P}}, t) \cdot f_i(\beta, Q^2)$$

G. Ingelman and P. Schlein, Phys. Lett. B **152** (1985) 256;

Flux factor

$$f_i^D(x, Q^2, x_{I\!P}, t) = f_{I\!P/p}(x_{I\!P}, t) \cdot f_i(\beta, Q^2)$$

$$f_{I\!P/p}(x_{I\!P}, t) = A_{I\!P} \cdot \frac{e^{B_{I\!P} t}}{x_{I\!P}^{2\alpha_{I\!P}(t)-1}}$$

$$\alpha_{I\!P}(t) = \alpha_{I\!P}(0) + \alpha'_{I\!P} t$$

The x_{IP} dependence is parametrised using a flux factor motivated by Regge theory.

The Pomeron trajectory is assumed to be linear.

$$f_i^D(x, Q^2, x_{I\!P}, t) = f_{I\!P/p}(x_{I\!P}, t) \cdot f_i(\beta, Q^2) + n_{I\!R} \cdot f_{I\!R/p}(x_{I\!P}, t) \cdot f_i^{I\!R}(\beta, Q^2)$$

G. Ingelman and P. Schlein, Phys. Lett. B **152** (1985) 256;

Pomeron Parton Distribution function

We step into the process of this project by performing a QCD fit under the same conditions and conventions as in H12006. We obtained almost identical result. Then we tried to vary Σ distribution functional form to improve our fitting procedure.

H1 parameterization form

$$z\Sigma(z,Q_0^2) = A_\Sigma z^{B_\Sigma}(1-z)^{C_\Sigma} e^{\frac{a=-0.01}{1-z}}$$

Fit A

$$zg(z,Q_0^2) = A_g(1-z)^{C_g} e^{\frac{a=-0.01}{1-z}}$$

Fit B

$$zg(z,Q_0^2) = A_g e^{\frac{a=-0.01}{1-z}}$$

Our form

$$z\Sigma(z,Q_0^2) = A_\Sigma z^{B_\Sigma}(1-z)^{C_\Sigma}\underbrace{(1+D_\Sigma z + E_\Sigma z^{F_\Sigma})}$$

Provides flexibility to obtain a good description of the data.

$$zg(z,Q_0^2) = A_g e^{\frac{a=-0.01}{1-z}}$$

It ensures that the distribution vanish at z=1, as required for evolution equation to be solvable.

A. Aktas *et al.* [H1 Collaboration], Eur. Phys. J. C **48**, 715 (2006) [arXiv:hep-ex/0606004].

Jet data is really urgent to constrain the gluon inside the DPDF.
The tool which experimental groups use for predictions is NLOJET++ adapted for diffraction. This Monte Carlo program however cannot be directly interfaced in a fit since it is very slowly. A possible way out is to use pre-calculated table obtained with FastNLO but unfortunately such a code/table doesn't exist at the moment. As soon as the FastNLO for diffractive jet data gets prepared, we include them in our analysis.

Data Analysis

How the data are presented

There is no unique definition of a cross section for DDIS. Different methods exist to select diffractive events. These methods select samples which contain different fractions of proton dissociative events. Cross sections are usually given without corrections for proton dissociation.

Three distinct methods have been employed by the HERA experiments, which select inclusive diffractive events.

FPS/LPS-LRG-M_X

Purpose: Direct measurement of the scattered proton
Measurement of t
Advantage: No p-diss background (**$M_Y=m_p$**)
Disadvantage: Low statistics due to the Roman Pot detector acceptance

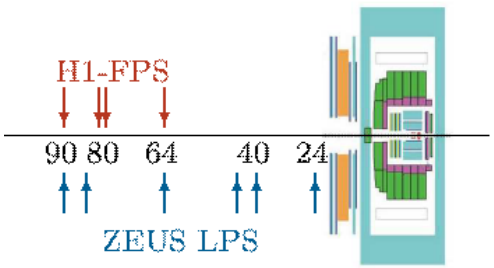

Require a large rapidity gap adjacent to the outgoing proton.
Escaping scattered proton cross section integrated over t
Advantage: Large statistics, large range in Q^2, x_{IP}, β
Disadvantage: Contamination of p-diss. (**M_Y<1.6 GeV**) & non diff. background

$$\eta = -ln[tan(\frac{\theta}{2})]$$

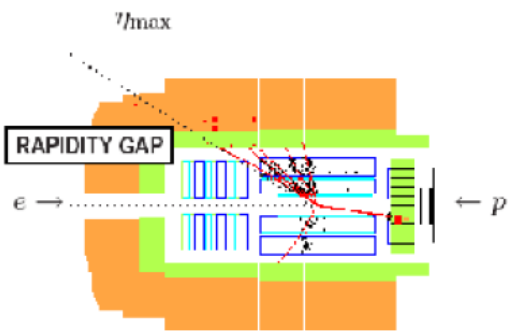

Require a large rapidity gap adjacent to the outgoing proton.
t measurement is nor possible
Advantage: Large statistics, No non diff. background
Disadvantage: Contamination of p-diss (**M_Y<2.3 GeV**)

$$\frac{dN}{d\ln M_x^2} = D + c\,e^{b\,\ln M_x^2}$$

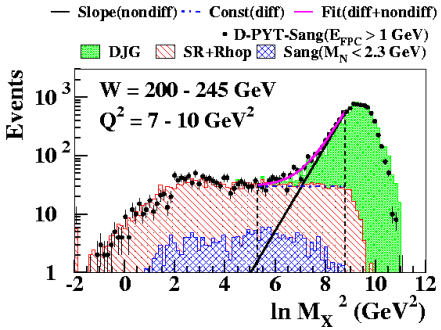

The full HERA data sample analysis is a powerful technique to achieve the best precision possible in extracting DPDFs. First steps are taken towards the combination of the H1 and ZEUS results. However, already at the present level, much can be done with existing data for the understanding of diffraction at HERA.
For all data and fit comparisons, all data are transported to the H1-LRG-06 measurement range $M_Y < 1.6$GeV.

- The first challenge is that M_X, used by ZEUS to separate diffractive from non diffractive events, and LRG methods use the same data and thus they are strongly correlated.

- Although the leading-proton data previously suffered from low statistics and hence were unlikely to have much influence on the fit results, the high statistics of the present data make them competitive in precision with the result of the LRG method.

- The LRG results from H1 and ZEUS are compatible in most of the kinematic region covered by measurements.

Our decision

1. No M_X data
2. FPS/LPS + LRG

P. Newman and M. Ruspa, arXiv:0903.2957 [hep-ex].

Published data points

Multiplying factor

	Lable	Data set	β-range	$x_{I\!P}$-range	Q^2-range	N_{Data}	$\mathcal{N}_i$
Reference →	H1-LRG-06	$\sigma_r^{D(3)}$	0.004-0.8	0.001-0.03	8.5-1600	190	0.9958
1.23 →	H1-FPS-06	$\sigma_r^{D(3)}$	0.02-0.7	0.0011-0.08	10.7-24	40	1.0023
1.20 →	H1-FPS-10	$\sigma_r^{D(3)}$	0.006-0.562	0.0025-0.075	8.8-200	100	1.0002
1.33 →	ZEUS-LPS-04	$F_2^{D(3)}$	0.007-0.48	0.0005-0.06	13.5-39	27	1.0005
1.33 →	ZEUS-LPS-09	$\sigma_r^{D(3)}$	0.013-0.609	0.0009-0.09	14-40	42	0.9845
1.05 →	ZEUS-LRG-09	$\sigma_r^{D(3)}$	0.025-0.795	0.0005-0.014	8.5-225	155	1.0094
0.97 →	H1-LRG-11	$F_{2,L}^{D(3)}$	0.089-0.699	0.0005-0.003	11.5-44	20	0.9739
0.99 →	H1-LRG-11	$\sigma_{r,(\sqrt{s}=225,252)}^{D(3)}$	0.089-0.699	0.0005-0.003	11.5-44	25	0.9739
0.97 →	H1-LRG-11	$\sigma_{r,(\sqrt{s}=319)}^{D(3)}$	0.089-0.699	0.0005-0.003	11.5-44	12	0.9608
1. →	H1-LRG-11	R^D	0.089-0.699	0.0005-0.003	11.5-44	10	1
	Total					621	

Table 1: Overview of the published data points for $\beta \leqslant 0.8$, $M_x > 2\,\mathrm{GeV}$ and $Q^2 \geqslant 8.5\ \mathrm{GeV}^2$ together with the fitted normalization shifts $\mathcal{N}_i$.

A. Aktas *et al.* [H1 Collaboration], Eur. Phys. J. C **48**, 715 (2006) [arXiv:hep-ex/0606004].

A. Aktas *et al.* [H1 Collaboration], Eur. Phys. J. C **48**, 749 (2006) [arXiv:hep-ex/0606003].

F. D. Aaron *et al.*, Eur. Phys. J. C **71**, 1578 (2011) [arXiv:1010.1476 [hep-ex]].

S. Chekanov *et al.* [ZEUS Collaboration], Nucl. Phys. B **713**, 3 (2005) [arXiv:hep-ex/0501060].

S. Chekanov [ZEUS Collaboration], Nucl. Phys. B **800**, 1 (2008) [arXiv:0802.3017 [hep-ex]].

H1. Collaboration, arXiv:1107.3420 [hep-ex].

Results

Our final results

Parameters	TKT
A_Σ	0.17 ± 0.009
B_Σ	0.08 ± 0.031
C_Σ	0.53 ± 0.025
D_Σ	4.88 ± 0.14
E_Σ	-2.36 ± 0.064
F_Σ	0.30 ± 0.012
A_g	0.44 ± 0.020
$\alpha_{I\!P}(0)$	1.108 ± 0.0035
$N_{I\!R}$(H1-LRG-06)	$(1.22 \pm 0.18) \times 10^{-3}$
$N_{I\!R}$(H1-FPS-06)	$(1.21 \pm 0.23) \times 10^{-3}$
$N_{I\!R}$(H1-FPS-10)	$(1.36 \pm 0.09) \times 10^{-3}$
$N_{I\!R}$(ZEUS-LPS-04)	$(1.64 \pm 0.26) \times 10^{-3}$
$N_{I\!R}$(ZEUS-LPS-09)	$(2.25 \pm 0.12) \times 10^{-3}$
$N_{I\!R}$(ZEUS-LRG-09)	$(2.19 \pm 0.29) \times 10^{-3}$
χ^2/dof	$601.92/607 = 0.99$

Table 2: Pomeron quark and gluon densities parameters and their statistical errors for combined data sets in $\overline{\mathrm{MS}}$ scheme at the input scale Q_0^2=3 GeV^2.

Our DPDFs

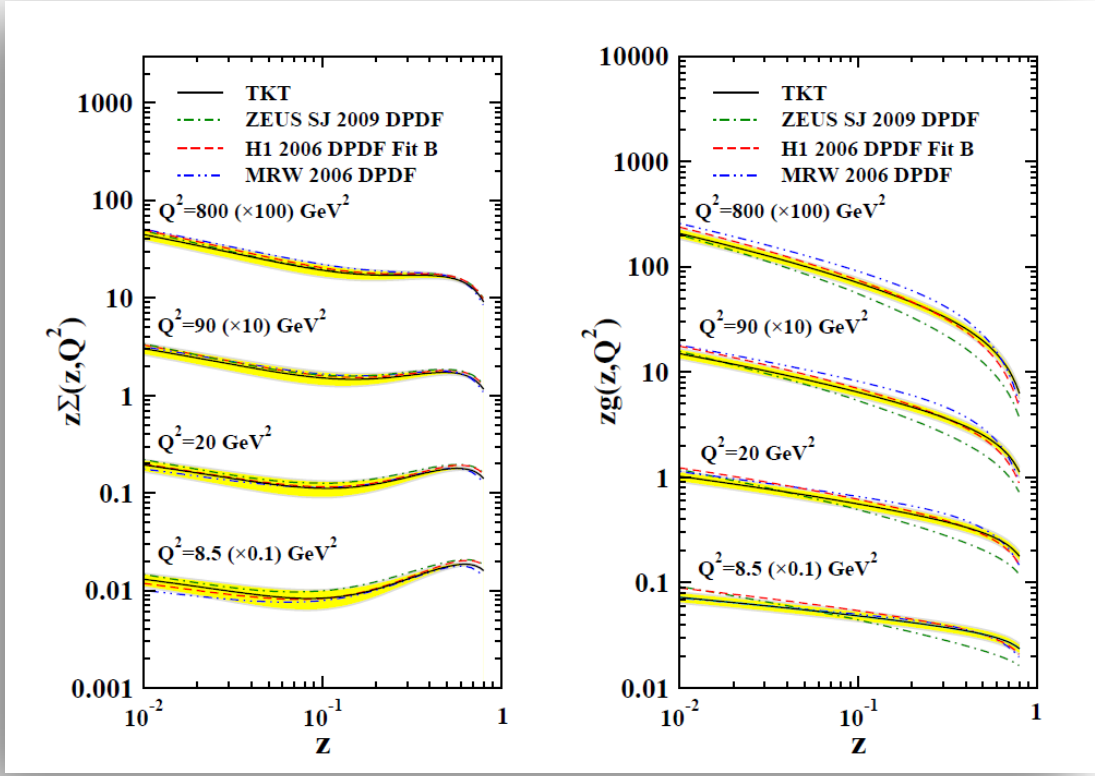

Figure 1: Comparison between the total quark singlet and gluon distributions obtained from our model, H1 2006 DPDF Fit B, ZEUS SJ and MRW at four different values of Q^2 as a function of z. The ZEUS SJ and MRW DPDFs plotted here are normalised to $M_Y < 1.6$ GeV by multiplying by a factor 1.23 relative to $M_Y = mp$.

Pion structure

The contribution of the sub-leading Reggeon trajectories should be considered for x_{IP} values substantially larger than 0.01. The contribution from these trajectories is modeled using the pion structure function. The pion PDFs are used in a region of low β where they are not directly constrained by data.. In order to limit the influence of sub-leading Reggeon trajectory, we exclude data points with $x_{IP} > 0.01$ and use a single N_{IR} for all required data sets. No significant difference exists between both fits showing the weak dependence of the fit on the precise knowledge on the Reggeon structure function.

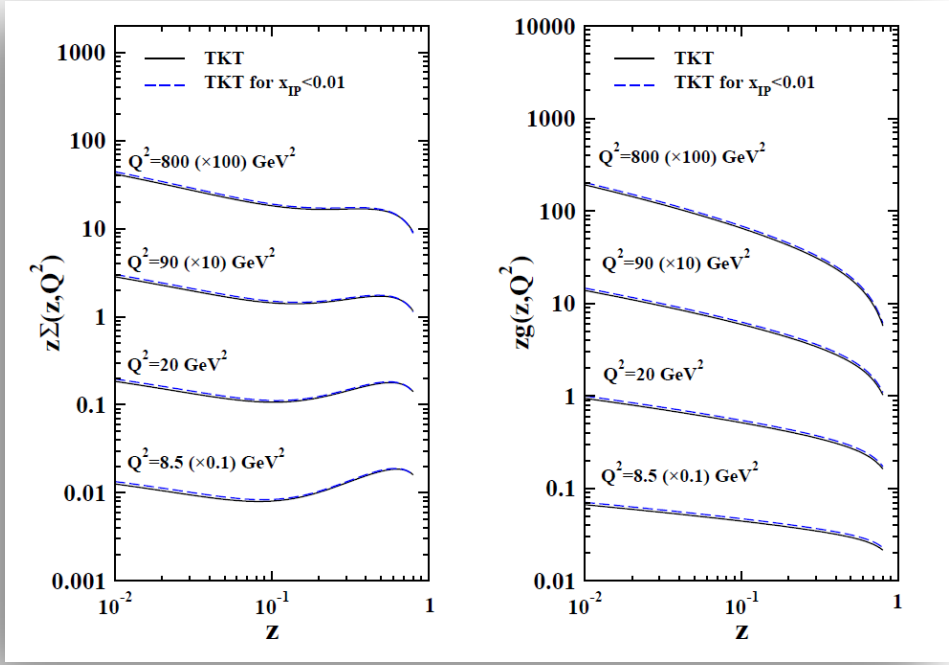

Figure 2: Comparison between the total quark singlet and gluon distributions obtained from our model. Results are presented with no cut on x_{IP} (solid) and x_{IP} < 0:01 (dashed).

Individual analysis

To study the degree of compatibility, we perform individual analysis on all data sets. It justifies our approach to combine all data sets.

Lable	χ^2/dof	Data points
H1-LRG-06	0.79	190
H1-FPS-06	0.53	40
H1-FPS-10	0.91	100
ZEUS-LPS-04	0.23	27
ZEUS-LPS-09	0.78	42
ZEUS-LRG-09	1.08	155
H1-LRG-11	0.89	67

Table 3: χ^2 values per data set for the gobal QCD fit with statistical and systematic errors added in quadrature.

S. Taheri Monfared, Ali N. Khorramian, S. Atashbar Tehrani, World Scientific, 503-510 (2010).

S. Taheri Monfared and A. N. Khorramian, Int. J. Mod. Phys. A **26**, 692 (2011).

S. Taheri Monfared, A. N. Khorramian, S. Atashbar Tehrani, J. Phys. Conf. Ser. **347** 012018 (2012).

Individual analysis

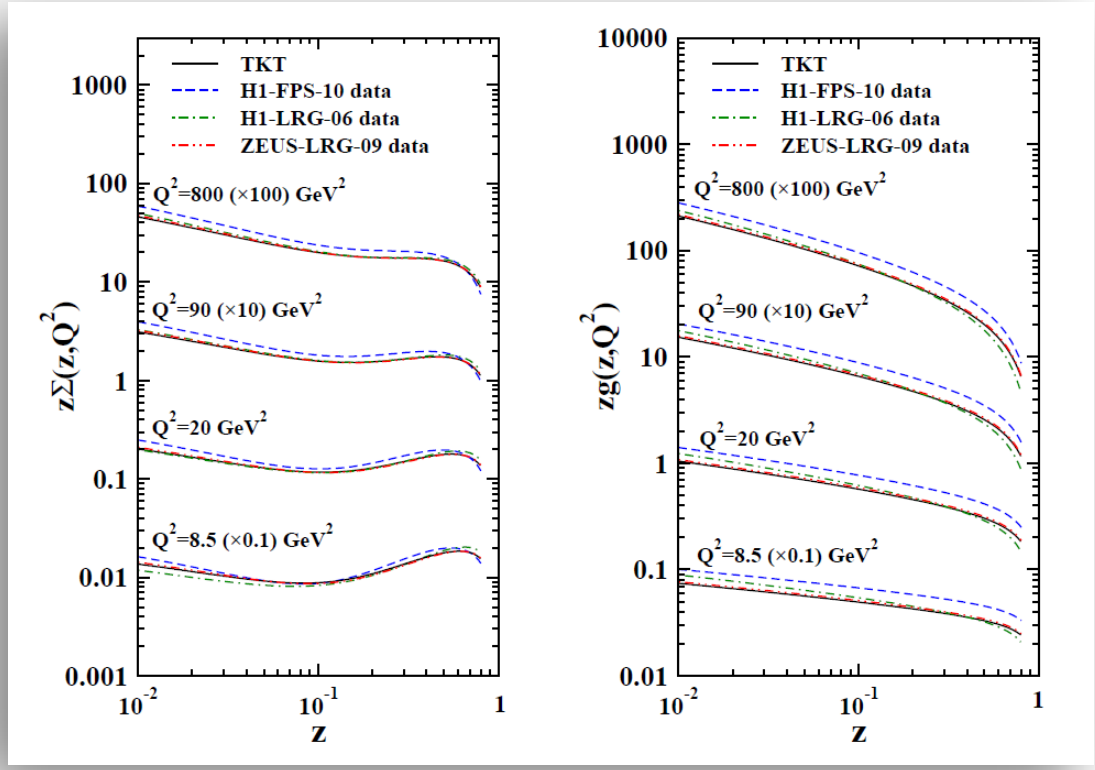

Figure 3: Singlet and gluon distributions of Pomeron as a function of z derived from QCD fits on H1-FPS-10 data alone, H1-LRG-06 data alone, ZEUS-LRG-09 data alone and all the data sets together.

Behaviour versus β

Cross section is largely flat in the measured β range. Keeping in mind the similarity between β in diffractive DIS and x_{Bj} in inclusive DIS, this is very different from the behavior of the usual cross section, which strongly decreases for $x_{Bj} > 0.2$.

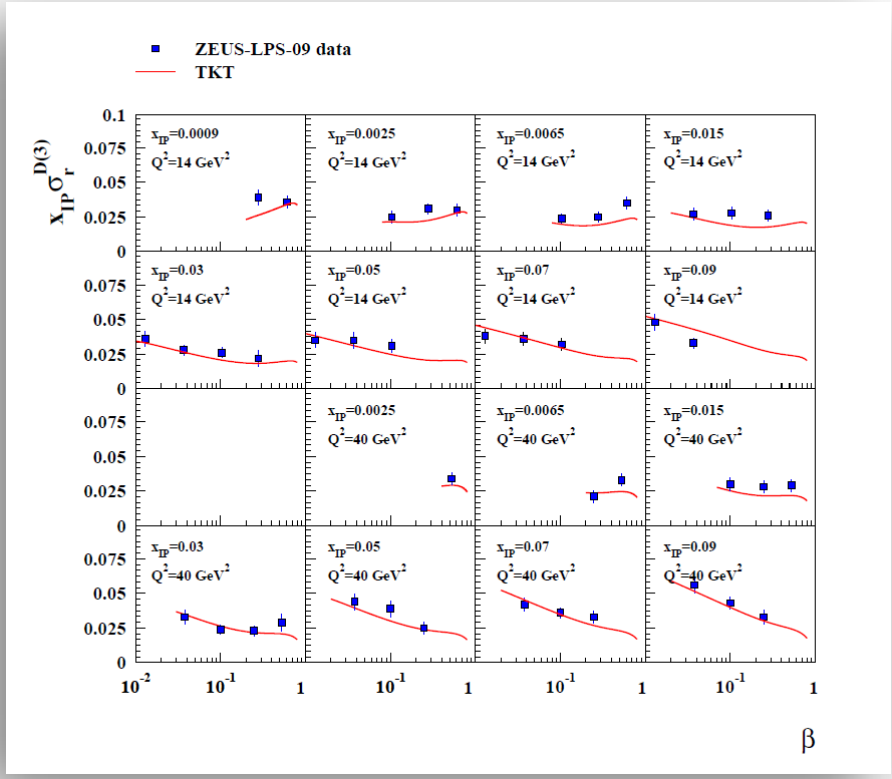

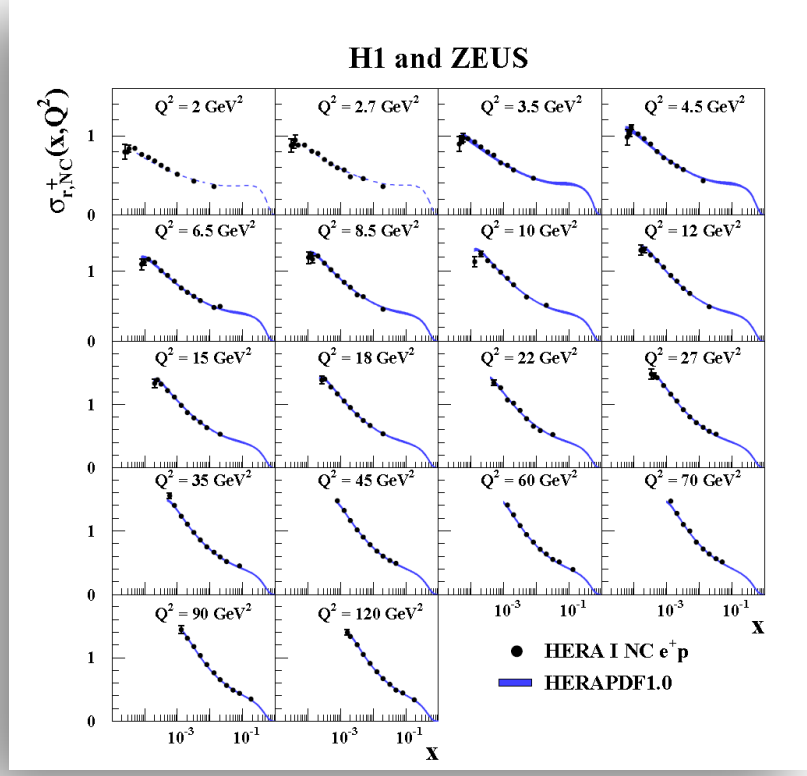

Figure 4: The ZEUS-LPS-09 $x_{IP}\sigma^{D(3)}$ as a function of β for different regions of Q^2 and x_{IP} . The curves show our model reduced by a global factor1.33 to correct for the contributions of proton dissociation processes.

F. D. Aaron *et al.* [H1 and ZEUS Collaboration], JHEP 1001, 109 (2010) [arXiv:0911.0884 [hep-ex]].

LRG data versus β

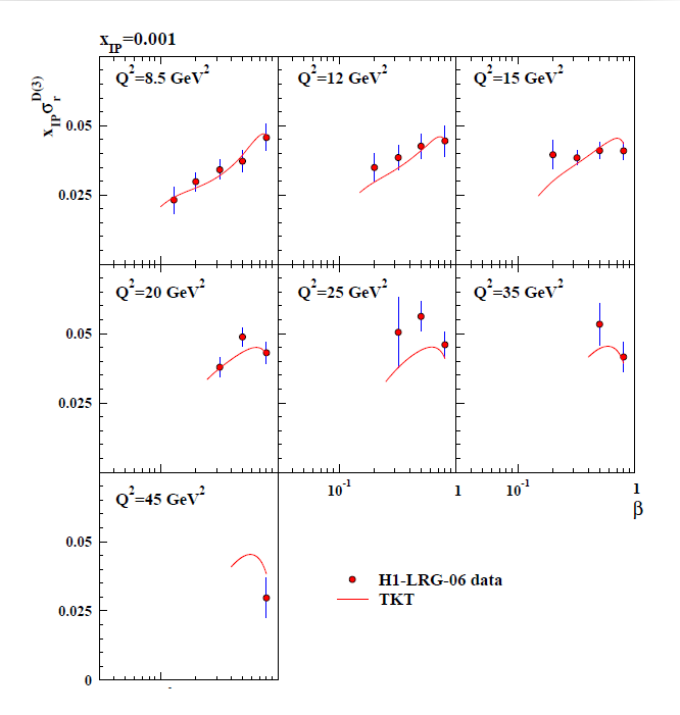

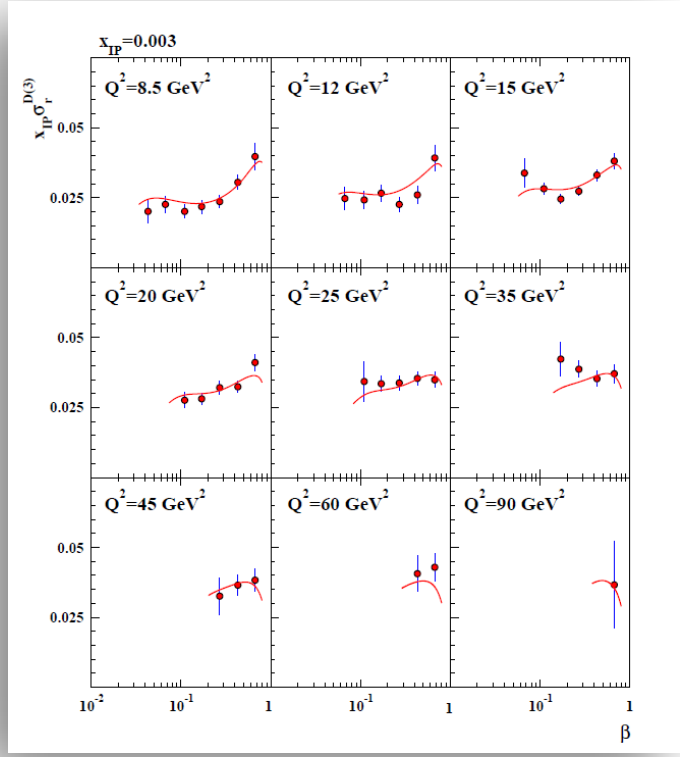

Figure 5: The H1-LRG-06 $x_{IP}\,\sigma^{D(3)}$ as a function of β for different regions of Q^2 and x_{IP} .

LRG data versus β

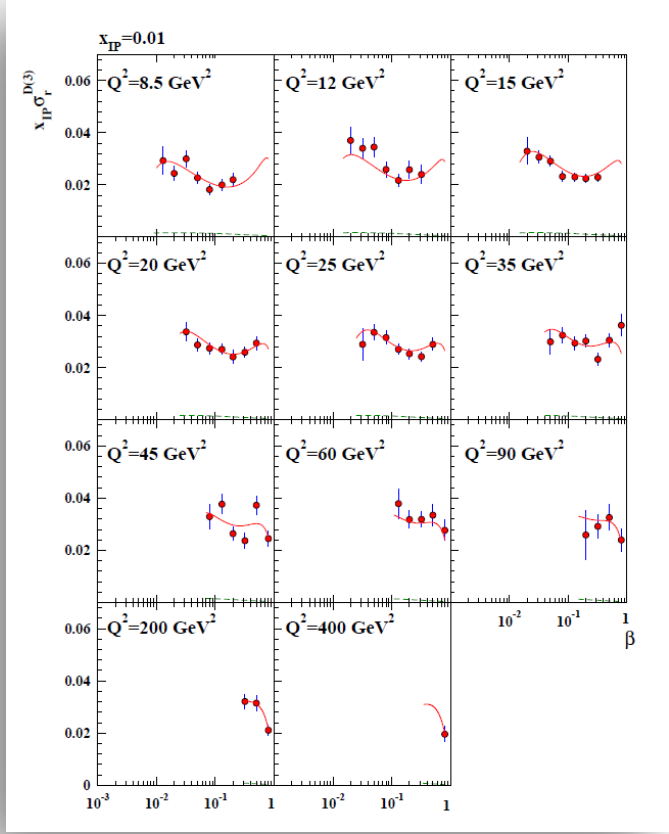

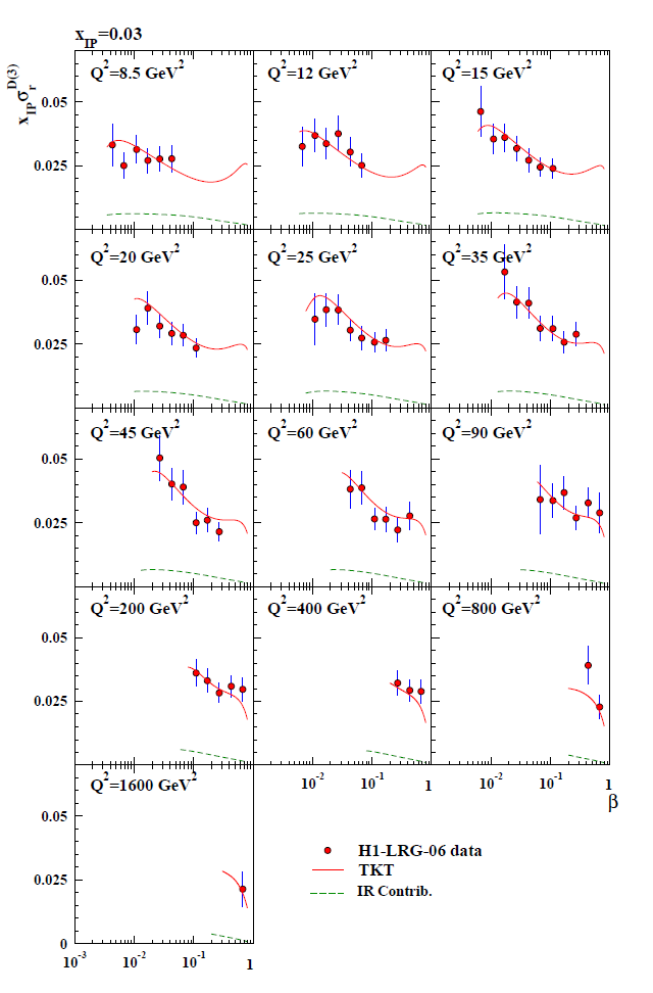

The contribution of the sub-leading exchange alone is also shown in x_{IP} = 0.03 and 0.01.

LRG data versus Q^2

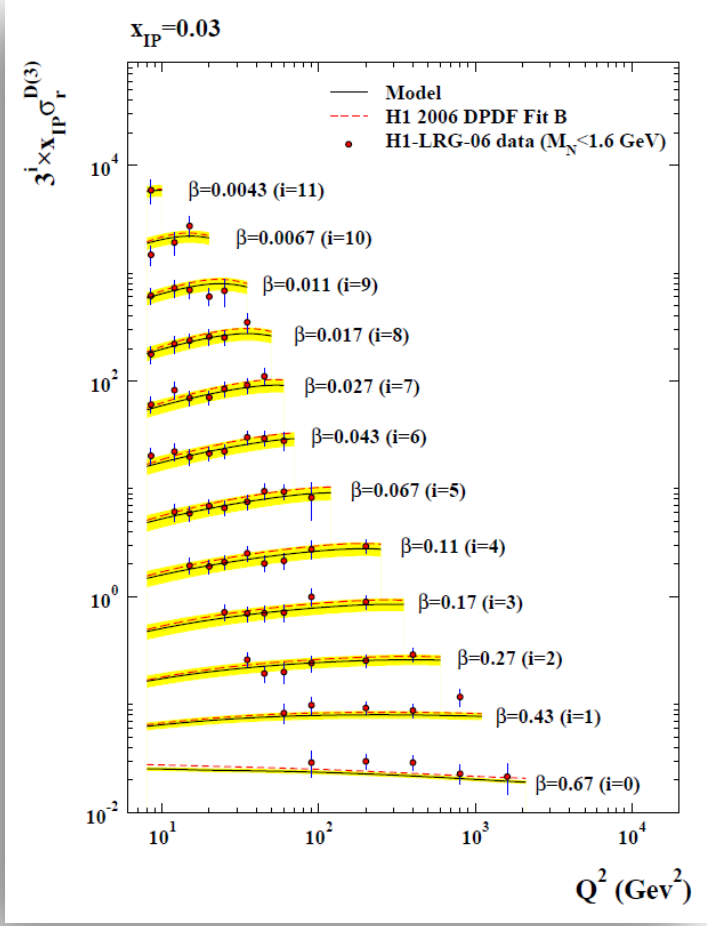

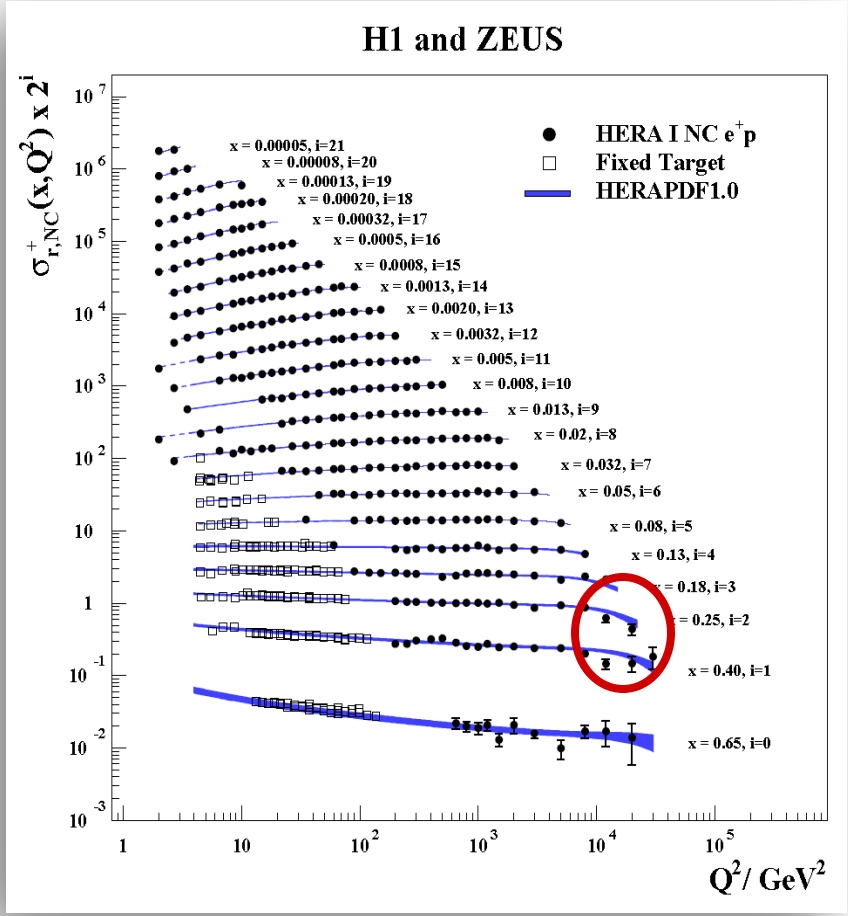

Positive scaling violations

are due to the growth of the sea quark and gluon densities

Negative scaling violations for x_{Bj}>0.2

manifest the existence of the valence quarks radiating gluons

F. D. Aaron *et al.* [H1 and ZEUS Collaboration], JHEP 1001, 109 (2010) [arXiv:0911.0884 [hep-ex]].

LRG data versus Q^2

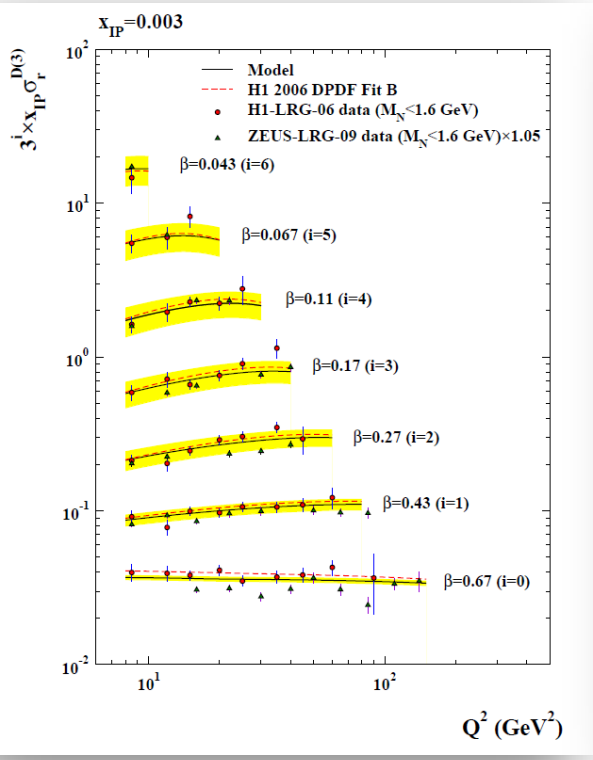

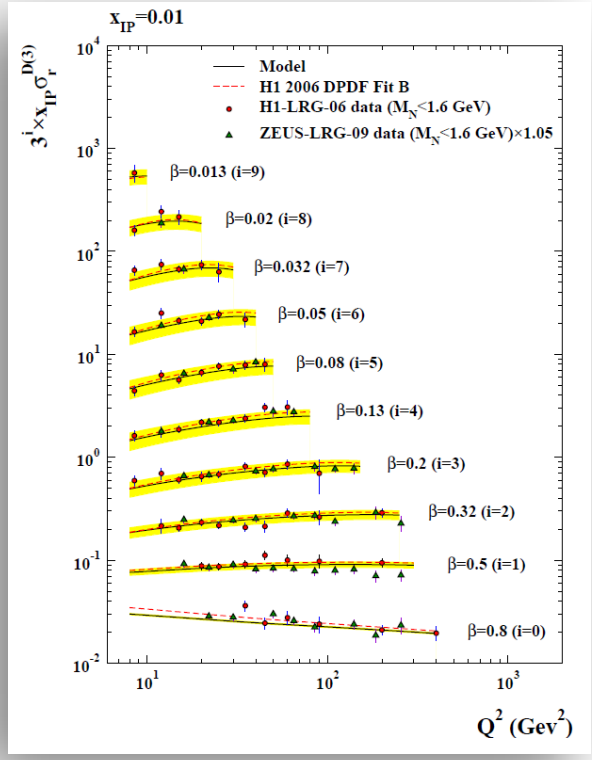

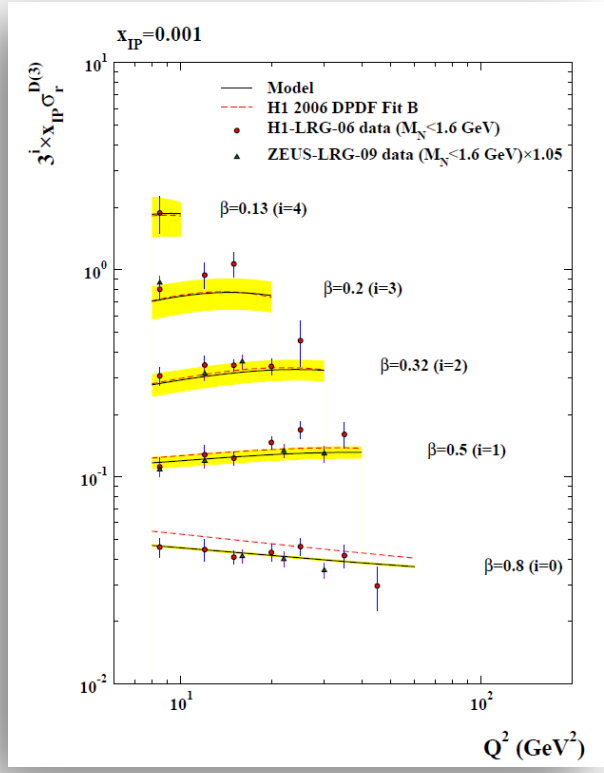

Figure 6: Comparison between the H1-LRG-06 and ZEUS-LRG-09 measurements after correcting the latter data set to $M_Y < 1.6$ GeV by applying scale factor of 1.05. The measurements are compared with our model and the results of the H1 2006 DPDF Fit B, which was based on the H1 data shown.

A. Aktas *et al.* [H1 Collaboration], Eur. Phys. J. C **48**, 715 (2006) [arXiv:hep-ex/0606004].

S. Chekanov [ZEUS Collaboration], Nucl. Phys. B **800**, 1 (2008) [arXiv:0802.3017 [hep-ex]].

ZEUS-LPS-04 data versus Q^2

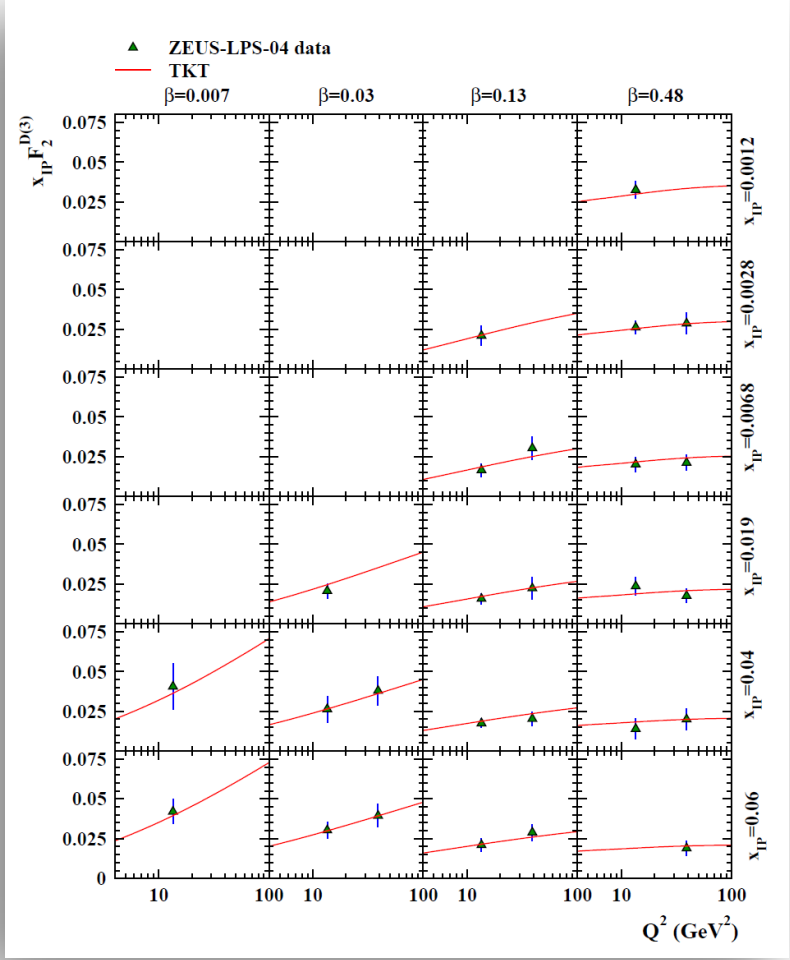

Figure 7 : $x_{IP}\,F_2^{D(3)}$, as a function of Q^2 for different regions of β and x_{IP}. Our model reduced by 1.33 to correct for the contributions of proton dissociation processes.

S. Chekanov *et al.* [ZEUS Collaboration], Eur. Phys. J. C **38**, 43 (2004) [arXiv:hep-ex/0408009].

H1-FPS-10 data versus Q^2

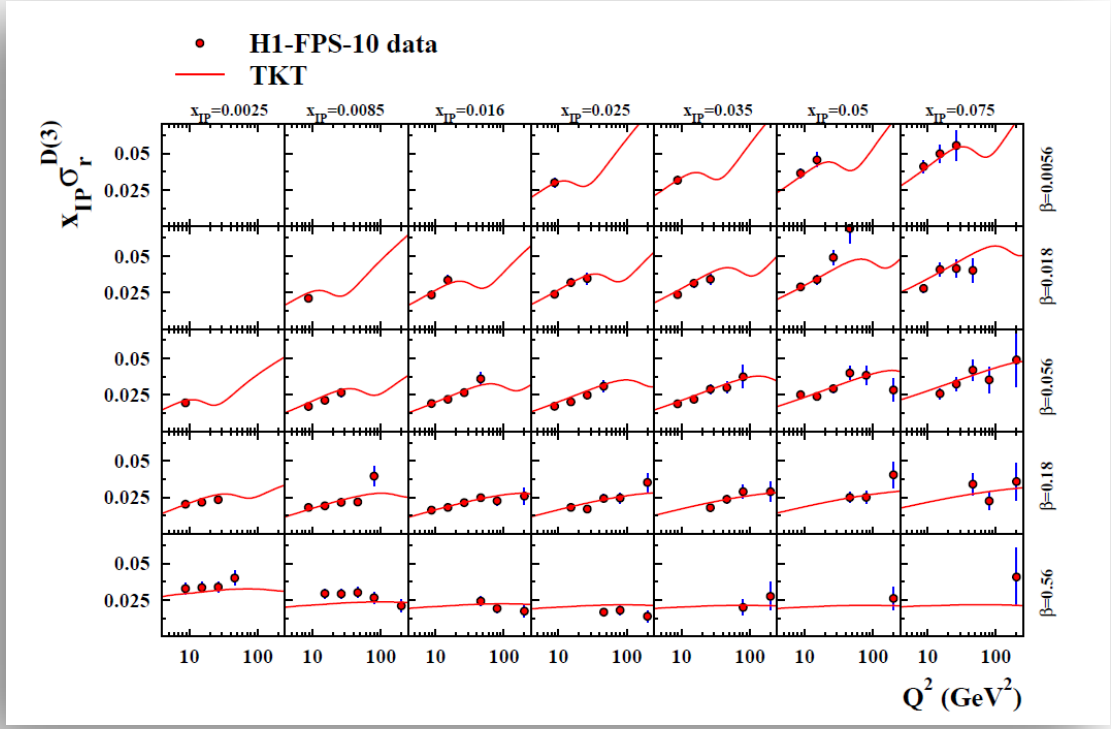

Figure 8: The diffractive cross section multiplied by x_{IP} , as a function of Q^2 for different regions of β and x_{IP}. The curves show our model reduced by a global factor 1.20 to correct for the contributions of proton dissociation processes as described previously.

H. Collaboration, arXiv:1010.1476 [hep-ex].

H1-FPS-06 data versus Q^2

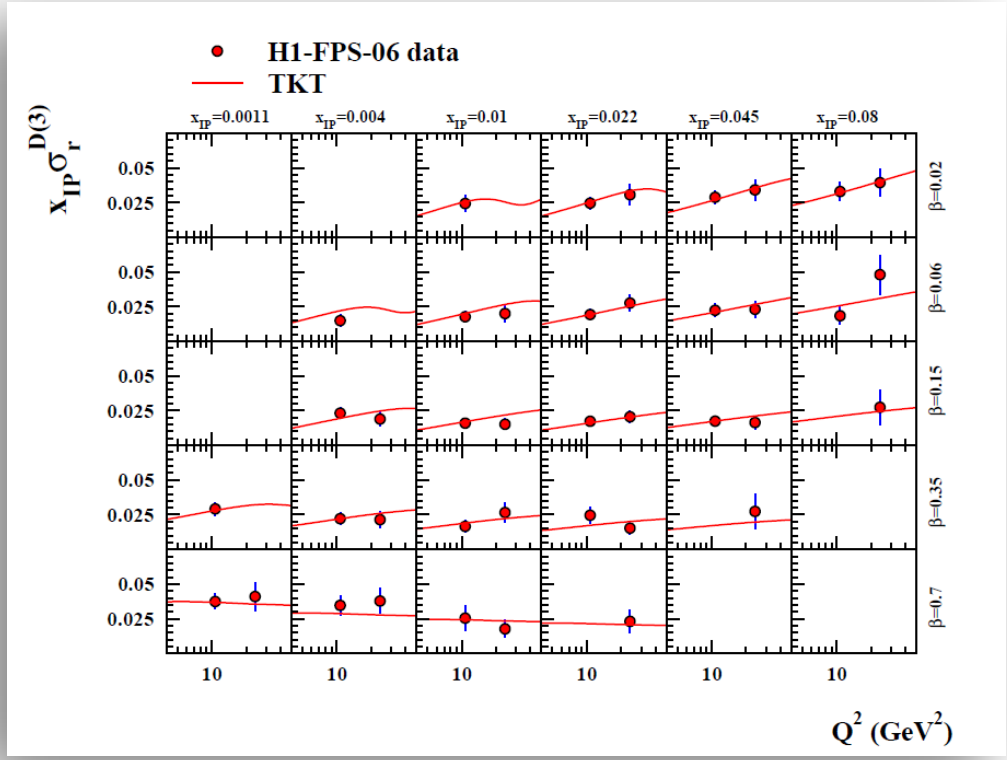

Figure 9: The diffractive cross section multiplied by x_{IP} , as a function of Q^2 for different regions of β and x_{IP}. The curves show our model reduced by a global factor 1.23 to correct for the contributions of proton dissociation processes as described previously.

A. Aktas *et al.* [H1 Collaboration], Eur. Phys. J. C **48**, 749 (2006) [arXiv:hep-ex/0606003].

ZEUS-M_X-08 data versus Q^2

We superimposed our results on M_X data. It shows that the fit can describe most kinematic regions. It leads to the conclusion that there seems to be compatibility between all data sets.

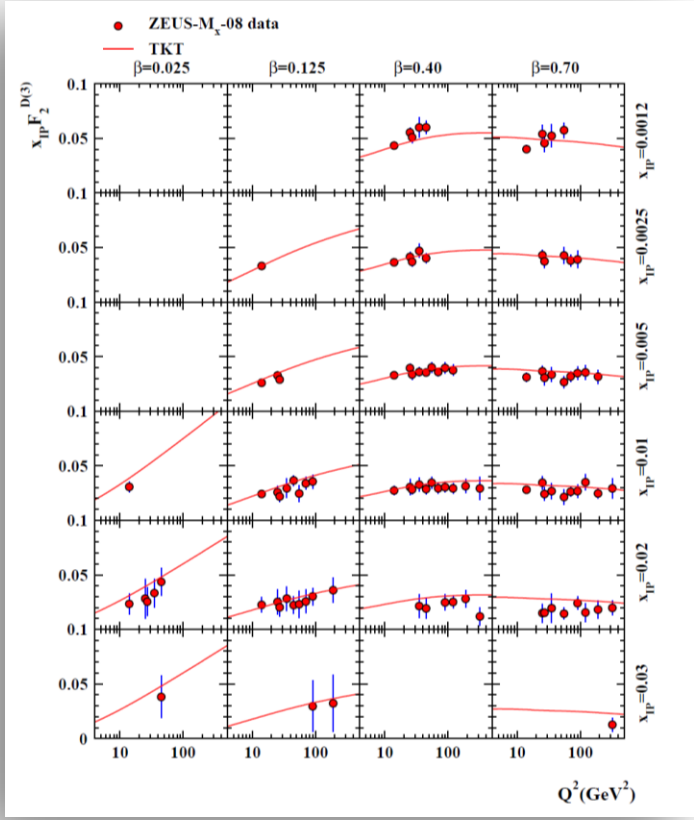

Figure 10: The diffractive cross section multiplied by x_{IP} , as a function of Q^2 for different regions of β and x_{IP}. The curves show our model reduced by a global factor 0.86 to correct for the contributions of proton dissociation processes as described previously.

S. Chekanov *et al.* [ZEUS Collaboration], Nucl. Phys. B **816**, 1 (2009) [arXiv:0812.2003 [hep-ex]].

ZEUS-M_X-05 data versus β

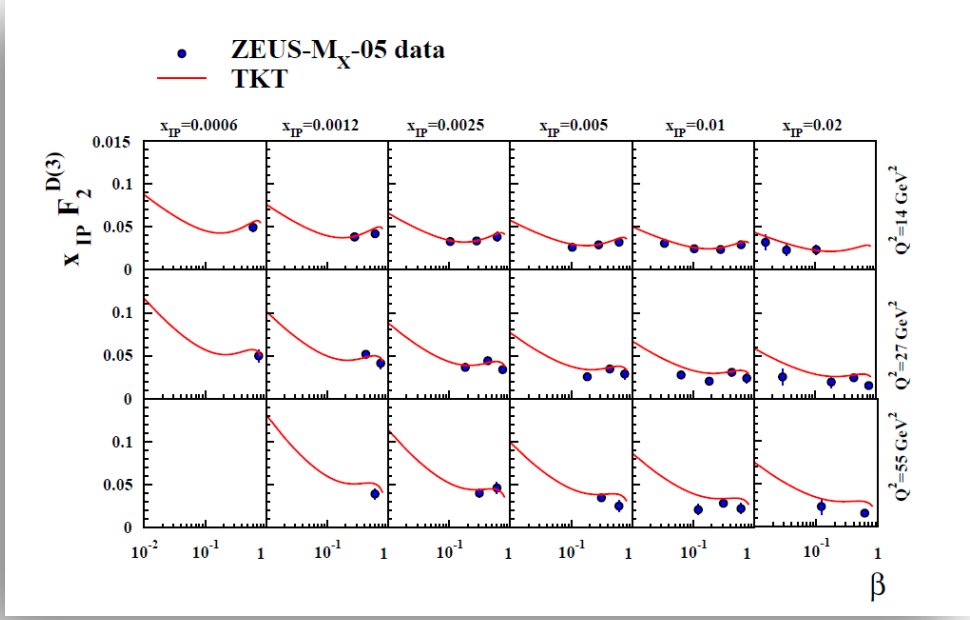

Figure 11: $x_{IP}\,\sigma_{D(3)}$, as a function of β at fixed Q^2 and x_{IP} for (from left to right) the 460, 575, 820 and 920 GeV data sets. The curves show our model reduced by a global factor 0.97, 0.99 and 0.97 for E_p=460, 575 and 920 GeV, respectively.

S. Chekanov *et al.* [ZEUS Collaboration], Eur. Phys. J. C **38**, 43 (2004) [arXiv:hep-ex/0408009].

Cross section on different E_P scales

A measurement of F_L^D provides a very powerful independent tool to verify our understanding of the underlying dynamics of diffraction and to test the DPDFs .
This is particularly important at the lowest β values, where direct information on the gluon density cannot be obtained via other methods.

The effect of diffractive F_L

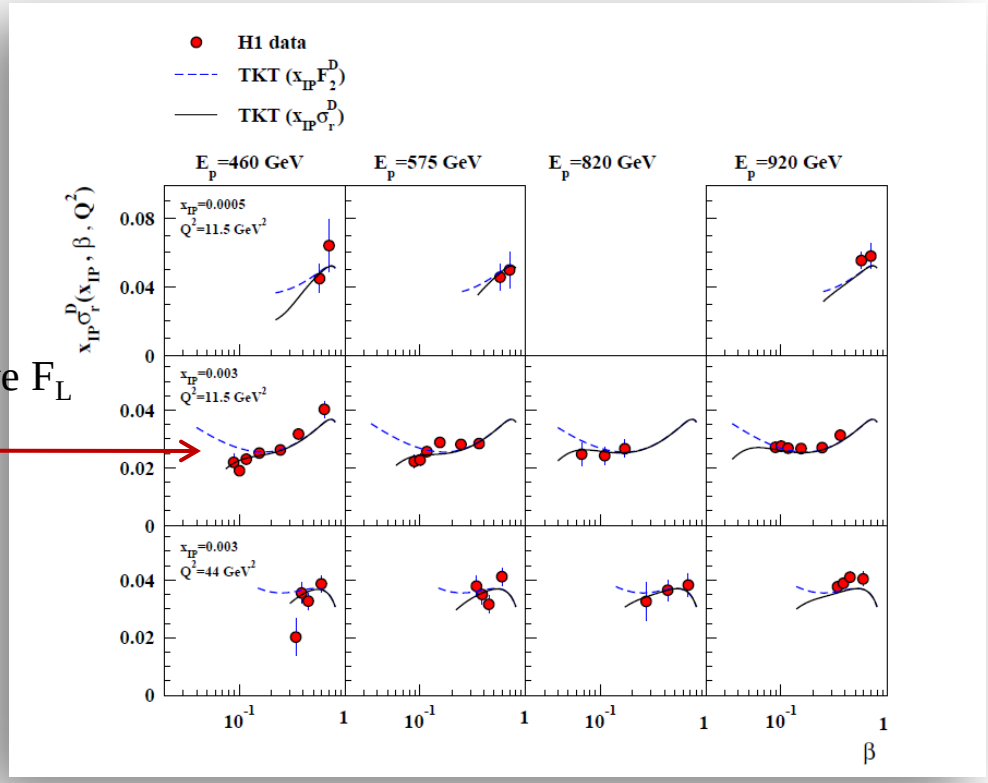

Figure 12: $x_{IP}\,\sigma_{D(3)}$, as a function of β at fixed Q^2 and x_{IP} for (from left to right) the 460, 575, 820 and 920 GeV data sets. The curves show our model reduced by a global factor 0.97, 0.99 and 0.97 for E_p=460, 575 and 920 GeV.

H1. Collaboration, arXiv:1107.3420 [hep-ex]

Only available data on diffractive F_L

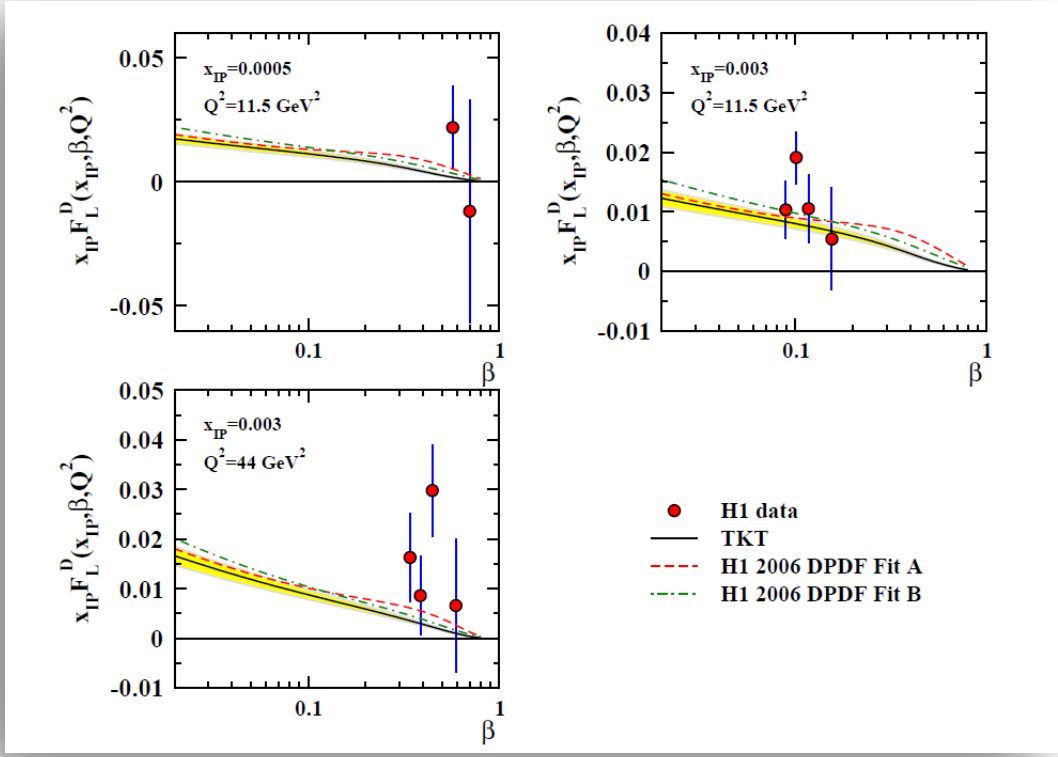

Figure 13: $x_{IP}F^D_L$ measurement as a function of β measured at fixed Q^2 and x_{IP} . The present fit is the solid curve. Also shown are the results of H1 2006 Fit A and and Fit B.

Ratio

$$R^D = F_L^D/(F_2^D - F_L^D)$$

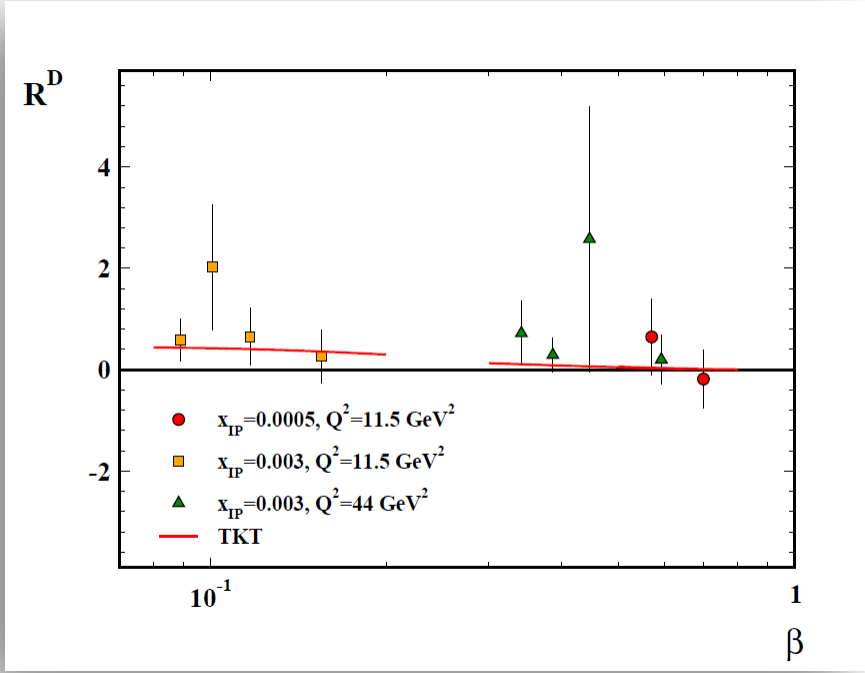

Figure 14: The ratio measurement, R_D, as a function of β at the indicated values of x_{IP} and Q^2. Our result is the solid curve.

Our result on charm cross sections and structure function

Charm production in diffractive DIS has been measured by H1 and ZEUS collaborations.
It allows quantitive tests of models due to the sensitivity of charm production to gluon density.

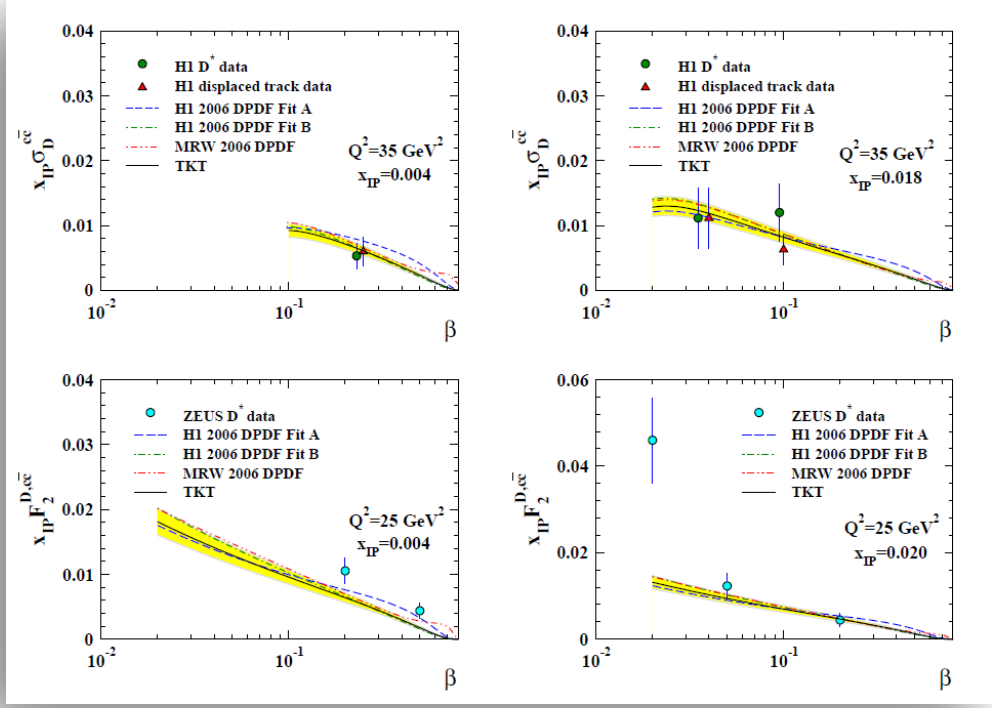

Figure 15: Comparison of our result for the contribution of the charm quarks to the diffractive cross section and structure function with H1 2006 DPDF Fit A, Fit B and MRW shown as a function of for different values of x_{IP} . The data obtained from the H1 and ZEUS D* production and from H1 displaced track method.

S. Chekanov *et al.* [ZEUS Collaboration], Nucl. Phys. B **672**, 3 (2003) [arXiv:hep-ex/0307068].

A. Aktas *et al.* [H1 Collaboration], Eur. Phys. J. C **50**, 1 (2007) [arXiv:hep-ex/0610076].

Conclusion

http://particles.ipm.ir/links/QCD.htm

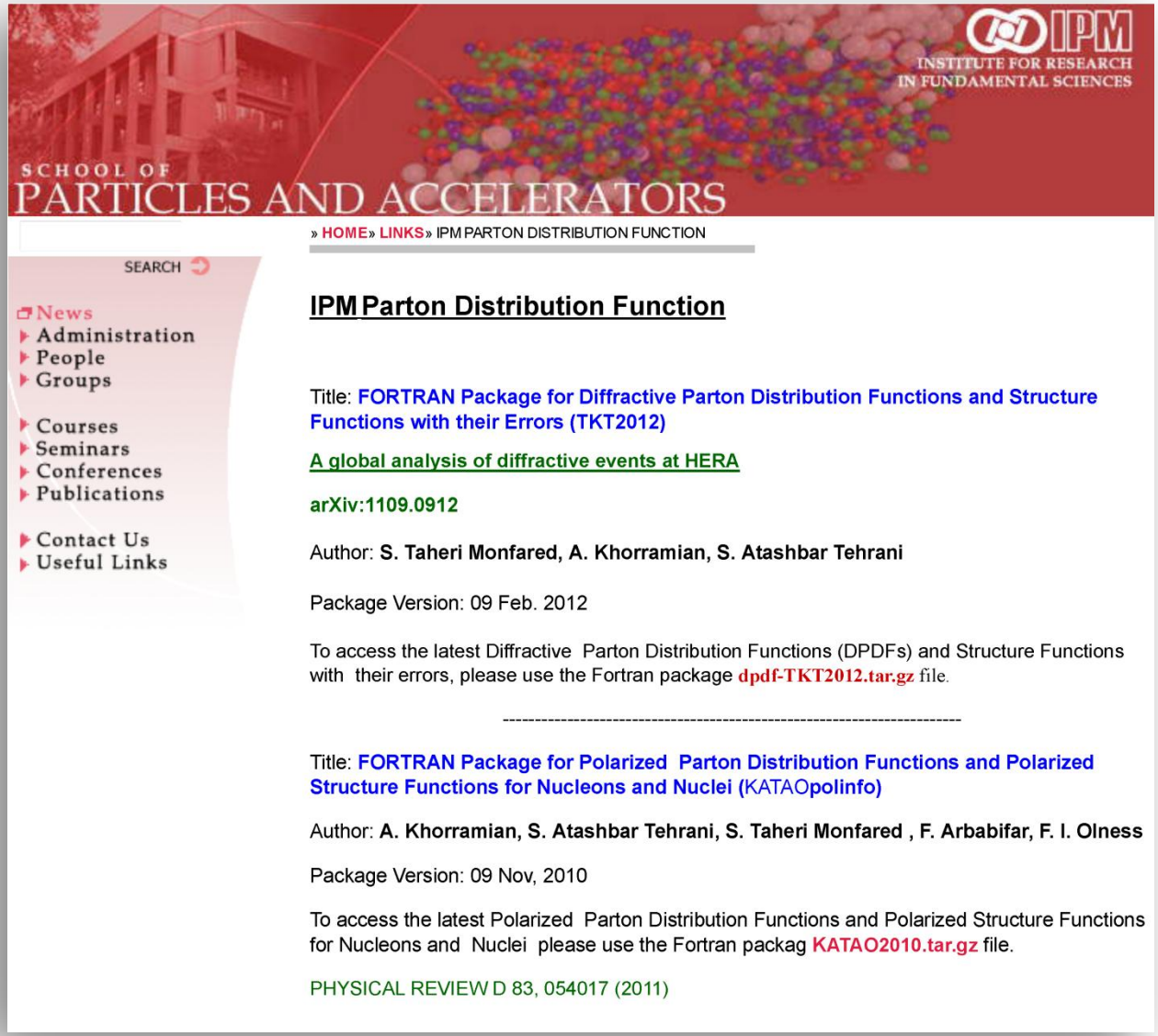

IPM
INSTITUTE FOR RESEARCH IN FUNDAMENTAL SCIENCES

SCHOOL OF
PARTICLES AND ACCELERATORS

» HOME» LINKS» IPM PARTON DISTRIBUTION FUNCTION

SEARCH

News
Administration
People
Groups

Courses
Seminars
Conferences
Publications

Contact Us
Useful Links

IPM Parton Distribution Function

Title: **FORTRAN Package for Diffractive Parton Distribution Functions and Structure Functions with their Errors (TKT2012)**

A global analysis of diffractive events at HERA

arXiv:1109.0912

Author: **S. Taheri Monfared, A. Khorramian, S. Atashbar Tehrani**

Package Version: 09 Feb. 2012

To access the latest Diffractive Parton Distribution Functions (DPDFs) and Structure Functions with their errors, please use the Fortran package **dpdf-TKT2012.tar.gz** file.

Title: **FORTRAN Package for Polarized Parton Distribution Functions and Polarized Structure Functions for Nucleons and Nuclei (**KATAO**polinfo)**

Author: **A. Khorramian, S. Atashbar Tehrani, S. Taheri Monfared , F. Arbabifar, F. I. Olness**

Package Version: 09 Nov, 2010

To access the latest Polarized Parton Distribution Functions and Polarized Structure Functions for Nucleons and Nuclei please use the Fortran packag **KATAO2010.tar.gz** file.

PHYSICAL REVIEW D 83, 054017 (2011)

Conclusion

In conclusion, this has been a general overview of what really fascinated me through the course of this study.

•We have shown that the diffractive observables measured in the H1 and ZEUS experiments at HERA can be well described by a perturbative QCD analysis which fundamental quark and gluon distributions, evolving according to the NLO DGLAP equations, are assigned to the Pomeron and Reggeon exchanges.

•We introduce new set of quark distribution which provide flexibility to obtain a proper description of the data.

•Although these data obtained by various methods with very different systematic, they are broadly consistent in the shape of the distribution. This is a very important message from HERA that diffractive DPDFs are well compatible for both experiments

• Our next steps are toward calculation of double diffractive phenomena in hadron–hadron colliders ...


Thanks for your paying attention

Light flavour contribution

Diffractive structure function to all order in perturbation theory can be described by

$$F_i(\beta, Q^2) = \sum_j C_i^j(\beta, \frac{Q^2}{\mu^2}) \otimes f_j(\beta, \mu^2) \ ,$$

Generally speaking, structure function can be written like

$$F_i(\beta, Q^2) = F_i^{light}(\beta, Q^2) + F_i^{heavy}(\beta, Q^2, m_h^2) \ .$$

$i = 2, L$

The flavor singlet contribution up to NLO is given by

$$\frac{1}{x} F_i^{light}(\beta, Q^2) = \frac{2}{9}\Big(C_{i,q} \otimes \Sigma + C_{i,g} \otimes g\Big)(\beta, Q^2),$$

NLO coefficient functions

M. Gluck, C. Pisano and E. Reya, Phys. Rev. D **77**, 074002 (2008) [Erratum-ibid. D **78**, 019902 (2008)] [arXiv:0711.1248 [hep-ph]].

W. L. van Neerven and A. Vogt, Nucl. Phys. B **588**, 345 (2000) [arXiv:hep-ph/0006154].

Heavy flavour contribution

The treatment of heavy quarks is something that nearly every group does slightly and it can lead to surprisingly different results for PDFs extracted.

- VFNS : p → (u, d, s, g) + (c, b, t)
- FFNS : p → (u, d, s, g)

$$F_i^h(\beta, Q^2) = \sum_k C_{i,k}^{FF,n_f}(Q^2/m_h^2) \otimes f_{i,k}^{n_f}(Q^2) \ .$$

$$z_{\max} = Q^2/(Q^2 + 4m^2)$$

$$\begin{aligned} F_k(\beta, Q^2, m^2) = & \frac{Q^2\alpha_s}{4\pi^2 m^2} \int_\beta^{z_{\max}} \frac{dz}{z} \Big[e_H^2 f_g(\frac{\beta}{z}, \mu^2) c_{k,g}^{(0)} \Big] \\ & + \frac{Q^2\alpha_s^2}{\pi m^2} \int_\beta^{z_{\max}} \frac{dz}{z} \Big[e_H^2 f_g(\frac{\beta}{z}, \mu^2)(c_{k,g}^{(1)} + \bar{c}_{k,g}^{(1)} \ln \frac{\mu^2}{m^2}) \\ & + \sum_{i=q,\bar{q}} \Big[e_H^2 \, f_i(\frac{\beta}{z}, \mu^2)(c_{k,i}^{(1)} + \bar{c}_{k,i}^{(1)} \ln \frac{\mu^2}{m^2}) \\ & + e_{L,i}^2 \, f_i(\frac{\beta}{z}, \mu^2)(d_{k,i}^{(1)} + \bar{d}_{k,i}^{(1)} \ln \frac{\mu^2}{m^2}) \Big] \Big] \ , \end{aligned}$$

$k = 2, L$

LO

NLO

A. D. Martin, W. J. Stirling, R. S. Thorne and G. Watt, Eur. Phys. J. C **63**, 189 (2009) [arXiv:0901.0002 [hep-ph]].

M. Gluck, E. Hoffmann and E. Reya, Z. Phys. C **13**, 119 (1982); M. Gluck, E. Reya and M. Stratmann, Nucl. Phys. B **422**, 37 (1994).

E. Laenen, S. Riemersma, J. Smith and W.L. van Neerven, Nucl. Phys. B **392** (1993) 162, 229; Phys. Lett. B **291** (1992) 325.

M. Gluck, P. Jimenez-Delgado, E. Reya and C. Schuck, Phys. Lett. B **664**, 133 (2008) [arXiv:0801.3618 [hep-ph]].

M. Gluck, P. Jimenez-Delgado and E. Reya, Eur. Phys. J. C **53**, 355 (2008) [arXiv:0709.0614 [hep-ph]].

M. Gluck, E. Reya and A. Vogt, Eur. Phys. J. C **5**, 461 (1998) [arXiv:hep-ph/9806404].

Non diffractive $$\frac{dN}{d\ln M_x^2} = c\,e^{b\,\ln M_x^2}$$

$$\frac{dN}{d\ln M_x^2} = D + c\,e^{b\,\ln M_x^2}$$

Diffractive $$\frac{dN}{d\ln M_x^2} \approx \text{const.} = D$$

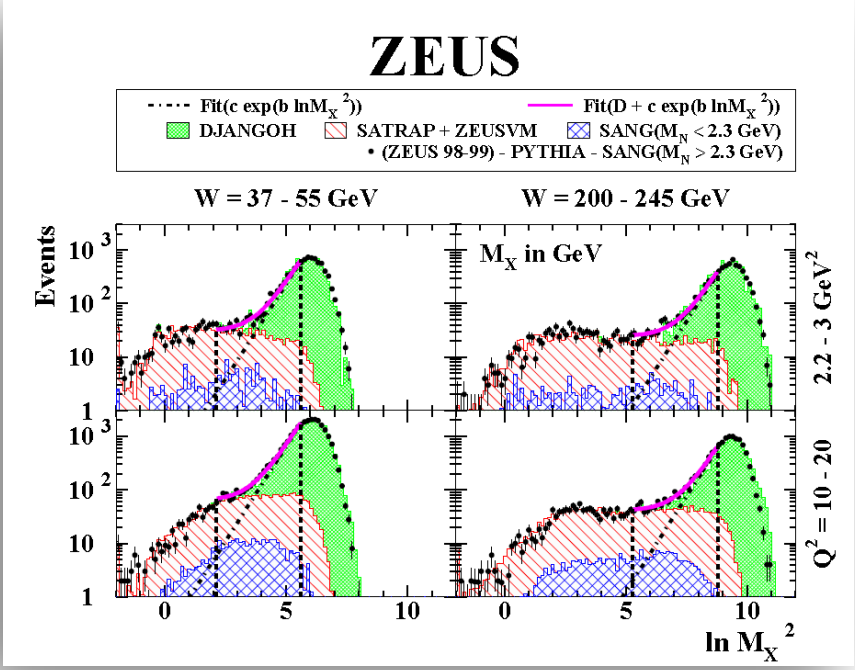

Error calculation

Overall normalization factor: obtained via first fit

Number of data points included

Data value

Theoretical value

$$\chi^2_{\text{global}}(p) = \sum_{i=1}^{n^{data}} \left[\left(\frac{1-\mathcal{N}_i}{\Delta \mathcal{N}_i} \right)^2 + \sum_{j=1}^{n^{data}} \left(\frac{\mathcal{N}_j \, F_{2,j}^{D,data} - F_{2,j}^{D,theor}(p)}{\mathcal{N}_j \, \Delta F_{2,j}^{D,data}} \right)^2 \right]$$

Set of independent parameters

Measurement uncertainty

Experimental normalization uncertainty: quoted by the experiments